Journal of Molecular Liquids 366 (2022) 120271

Contents lists available at ScienceDirect

Journal of Molecular Liquids

journal homepage: www.elsevier.com/locate/molliq

Tribological enhancement using Mn_3O_4-Graphene nanocomposites as additives for potential transmission fluids of electric vehicles

José M. Liñeira del Río [a,b,*], Ramón Rial [c], Enriqueta R. López [a], Josefa Fernández [a]

[a] Laboratory of Thermophysical and Tribological Properties, Nafomat Group, Department of Applied Physics, Faculty of Physics and Institute of Materials (iMATUS), Universidade de Santiago de Compostela, 15782, Santiago de Compostela, Spain
[b] Unidade de tribologia, vibraçoes e manutençao industrial, INEGI, Universidade do Porto, Porto, Portugal
[c] Soft Matter and Molecular Biophysics Group, Department of Applied Physics, Faculty of Physics and Institute of Materials (iMATUS), University of Santiago de Compostela, 15782 Santiago, Spain

ARTICLE INFO

Article history:
Received 7 June 2022
Revised 1 August 2022
Accepted 31 August 2022
Available online 5 September 2022

Keywords:
Transmission fluids
Nanocomposites
Electric vehicles
Tribological mechanisms
Friction
Wear

ABSTRACT

This research reports the antifriction and antiwear properties of Mn_3O_4-Graphene nanocomposites (Mn_3O_4-G) as additives of a paraffinic base oil commonly used in the formulation of electric vehicles transmission oils, G-III base oil. Four G-III base oil nanodispersions have been designed, G-III base oil + 0.025 wt% Mn_3O_4-G, G-III base oil + 0.050 wt% Mn_3O_4-G, G-III base oil + 0.075 wt% Mn_3O_4-G and G-III base oil + 0.100 wt% Mn_3O_4-G, to know the optimal concentration of nanoadditive. Tribological experiments were carried out with these nanolubricants and with neat G-III base oil at pure sliding conditions under a working load of 9.43 N. All tested nanolubricants led to similar friction coefficients in comparison to that obtained using G-III base oil. Tribological specimens tested with formulated nanolubricants revealed less wear than that obtained with G-III base oil, obtaining the greatest wear reduction using the G-III base oil + 0.075 wt% Mn_3O_4-G nanolubricant, with reductions of 25, 50 and 64% in wear scar diameter, maximum depth and transversal area, respectively. Moreover, by means of confocal Raman microscopy and roughness evaluation of worn tribological specimens, it was concluded that synergetic effect, tribofilm formation and rolling mechanisms happen.
© 2022 The Authors. Published by Elsevier B.V. This is an open access article under the CC BY license (http://creativecommons.org/licenses/by/4.0/).

1. Introduction

Energy demands are continuously growing, with a special concern for the environment and climate change. Friction consumes about 20 % of all energy used worldwide [1]. Furthermore, the transport sector, traditionally driven by combustion technologies, is responsible for a large part of CO_2 emissions and one of the main contributors to climate change. Environmental issues and the excessive use of fossil fuels, have brought electric vehicles (EVs) to the head of automotive research [2]. When electricity generation is shifted from fossil power to renewable or nuclear powers, the environment benefits of electric vehicles are enormous: near 77 percent reduction in CO_2 emissions footprint according with recent cradle-to-grave calculations. In addition, Holmberg et al. [1,3] reported that only around 22% from the total fuel energy provided to the combustion engine, is utilized to push the vehicle, whereas EVs use for the same purpose around 77 % of the total energy taken from the electrical grid [1]. Through years of combined progress efforts, lubricants for vehicles with internal combustion engines (ICEs) have been improved and new efficiency challenges for electric mobility must now be addressed. Being so efficient and producing very few emissions, the efficiency and durability problems of electric cars focus on the moving parts and, therefore, on their tribology. By reducing friction in components such as rolling bearings and gears, tribology can help extend the driving range of electric vehicles. In many of the hybrid electric vehicles (HEV) and EV hardware designs, automatic transmission fluids are in contact with the incorporated electric motor that requires thermal and electrical properties to be considered in addition to conventional fluid properties [4]. Hence, compared to conventional ICE vehicles, mechanical components of EVs operate at higher speeds, loads, and temperatures [5]. This requires a low-viscosity lubricant with good thermal properties for efficient heat removal. The performance of low-viscosity lubricants can be retained by developing additive technology with several functions, for instance, simultaneous anti-wear and friction-reducing properties. To meet the recommended requirements for future EV lubricants, it is necessary to use advanced additives [6]. Nanotechnology based anti-wear and anti-friction additives and ionic liquid additives have been pro-

* Corresponding author.
E-mail address: josemanuel.lineira@usc.es (J.M. Liñeira del Río).

https://doi.org/10.1016/j.molliq.2022.120271
0167-7322/© 2022 The Authors. Published by Elsevier B.V.
This is an open access article under the CC BY license (http://creativecommons.org/licenses/by/4.0/).

posed for transmission fluids for EVs [7]. As several nanoadditives have shown excellent anti-friction and anti-wear capabilities, as well as a high thermal conductivity, they can help in the development of a new generation of low-viscosity lubricants specially adapted to the working conditions of the transmission fluids of electrified drivelines of EVs [5,6,8]. Moreover, nanoadditives are environmentally friendly in comparison to other traditional additives [9–11]. Although nanolubricants have demonstrated success in decreasing the friction and wear in traditional lubricants [8,12–15], there are hardly any research on nanolubricants in terms of EVs' tribological requirements. Mustafa et al. [16] reviewed the tribological behavior of some low-viscosity lubricants, based on PAO6, PAO8, PAO10 and water. For example, Kalin et al. [17] analyzed the tribological performance of a PAO6 nanolubricant containing MoS_2 nanotubes as additives, finding an important improvement in friction and wear, respect to the base oil.

Given the aforementioned needs, it is necessary to develop and investigate potential lubricants composed by low-viscosity base oils and nanomaterials as additives. In this research, the main aim is to characterize the tribological performance of trimanganese tetraoxide-graphene nanocomposites (Mn_3O_4-G) as hybrid additives for a low-viscosity paraffinic base oil (G-III base oil). This oil was obtained by an isodewaxing process which guarantees very low levels of sulphur (<10 ppm) and aromatic compounds. It is a very high viscosity index (VHVI) oil, classified as an API Group III, and as a 1-a in copper corrosion tests (ASTM D130) [18]. Mn_3O_4-G nanocomposites were chosen as additives owing to their potential cooperative and synergetic effect to improve the tribological behavior of 2D graphene nanosheets as lubricant additives and because the Mn_3O_4 nanoparticles (NPs) presence in the graphene layers can weaken the close contact between them inhibiting the agglomeration in the oil [19]. For instance, Zhao et al. [19] observed outstanding tribological properties owing to a synergistic lubrication effect among the graphene nanosheets and the Mn_3O_4 NPs in PAO6 base oil. These authors suggested that the Mn_3O_4 NPs can separate the graphene layers and improve the tribological performance through "slide–roll" effects. Furthermore, Jin et al. [20] analyzed the tribological performance of Mn_3O_4-Graphene nanocomposites as additives of a grease, observing also friction and wear reductions.

Therefore, because there is not much research on nanocomposites as low-viscosity oil additives, other than polyalphaolefins, this paper proposes a tribological study of a specific paraffinic-type oil (less common than PAOs) with Mn_3O_4 nanoadditives. To the knowledge of the authors, there are no articles that study the tribological performance of low-viscosity paraffinic oils using Mn_3O_4 additives.

2. Materials and methods

2.1. Materials

The G-III base oil sample was supplied by Repsol S.A. (Spain), has a dynamic viscosity and a density at 313.15 K of 28.85 mPa and 0.8234 g·cm^{-3}, respectively, and a very high viscosity index (133.3). This sample was characterized by means of infrared spectroscopy (FTIR) and Raman spectroscopy. Fig. 1 shows the FTIR spectrum, revealing the following characteristic peaks: around 2950 cm^{-1}, 2920 cm^{-1} and 2850 cm^{-1} associated to carbon-hydrogen groups: CH_3 asymmetric stretching, CH_2 asymmetric stretching and CH_3 symmetric stretching, respectively [21], at 1460 cm^{-1} a strong methylene/methyl band, at 1375 cm^{-1} a weak methyl band and at 720 cm^{-1} a peak associated to the methylene rocking vibration, which indicates the presence of long-chain linear aliphatic structure [22].

Regarding the Raman spectrum, Fig. 2 shows mainly the following bands: around 1300–1600 cm^{-1} due to the bond C—C stretching, and at 2900–3000 cm^{-1} owing to the C—H stretching.

Mn_3O_4-Graphene nanocomposite, Mn_3O_4-G, (proportion 1:1) was supplied by US Research Nanomaterials, Inc. (Houston, TX USA). Graphene has a purity > 99.5%, thickness in the range of (0.35–1.2) nm and size of 1–10 μm. Mn_3O_4 NPs, also with a purity > 99.5%, have an average particle size of 30 nm. Scanning electron microscope (SEM, Zeiss FESEM Ultra Plus) was used to describe the appearance and dimension of both nanomaterials in the nanocomposite. As can be observed in Fig. 3, in the nanocomposite the Mn_3O_4 NPs have spherical shape and are placed between the graphene nanosheets. The typical laminar layers of graphene are also shown. Furthermore, Fig. 3 confirms the sizes of the Mn_3O_4 NPs and graphene provided by the supplier.

Moreover, Mn_3O_4-G has also been characterized through FTIR. Fig. 4 shows the characteristic peak of the Mn—O stretching modes at 580 cm^{-1} [23]. It is also depicted the characteristic peaks of graphene derivatives located at 3400 cm^{-1} due to O—H stretching vibrations, at 2920 cm^{-1} associated to the C—H stretching, at 1660 cm^{-1} due to C═O stretching vibrations and at 1080 cm^{-1} owing to C—O stretching vibrations [24]. These functional groups are linked to the graphene structure as a result of the synthesis process.

Concerning the Raman characterization of Mn_3O_4-G nanocomposite, the spectrum at 532 nm (Fig. 5) shows the characteristic absorption bands of Mn—O vibrations at 649 cm^{-1} [25]. Furthermore, typical graphene Raman bands can be also observed in Fig. 5: D-band at 1355 cm^{-1}, G-band around 1570 cm^{-1} and G′-band around 2700 cm^{-1} [26,27]. From the Figure S1deconvolution of 2D band, it is clear that this band has a two-peak profile, the intense 2D1 band and a low energy shoulder called 2D2 band. In comparison with the Raman spectra of graphene with different layers [26,28] it can be concluded that the nanocomposite contains around five layers-graphene. As expected, typical bands of each nanocomposite component (Mn_3O_4 and Graphene) are present in the Raman spectrum of the nanocomposite.

Finally, Mn_3O_4-G nanocomposite was characterized by X-ray diffraction (XRD) to obtain information about the crystalline structure. Fig. 6 shows the XRD pattern of the Mn_3O_4-G nanocomposite. It can be observed that the characteristic diffraction peaks are consistent with the standard Mn_3O_4 spectrum, *i.e.*, 2θ = 18.011°, 28.952°, 32.298°, 36.097°, and 59.864° [29]. All these peaks can be classified in Hausmannite Mn_3O_4 (JCPDS no. 76–1650) [30]. Furthermore, the presence of an intense peak at 26.6° should be associated to graphene layers [31].

2.2. Design of nanodispersions

Nanolubricants were prepared following the traditional two-step method. The dry nanocomposites were combined with G-III base oil utilizing a Sartorius MC 210P balance (readability of 0.01 mg) to obtain the required concentrations. Next, nanodispersions homogenization was achieved using an ultrasonic bath during 4 h. To know which is the optimal concentration that leads to the best tribological performance, the following nanodispersions were made: G-III base oil + 0.025 wt% Mn_3O_4-G, G-III base oil + 0.050 wt% Mn_3O_4-G, G-III base oil + 0.075 wt% Mn_3O_4-G and G-III base oil + 0.100 wt% Mn_3O_4-G.

2.3. Friction tests and wear evaluation

Ball-on-three pins tribological tests with G-III base oil and with the Mn_3O_4-G nanolubricants were carried out using a Peltier

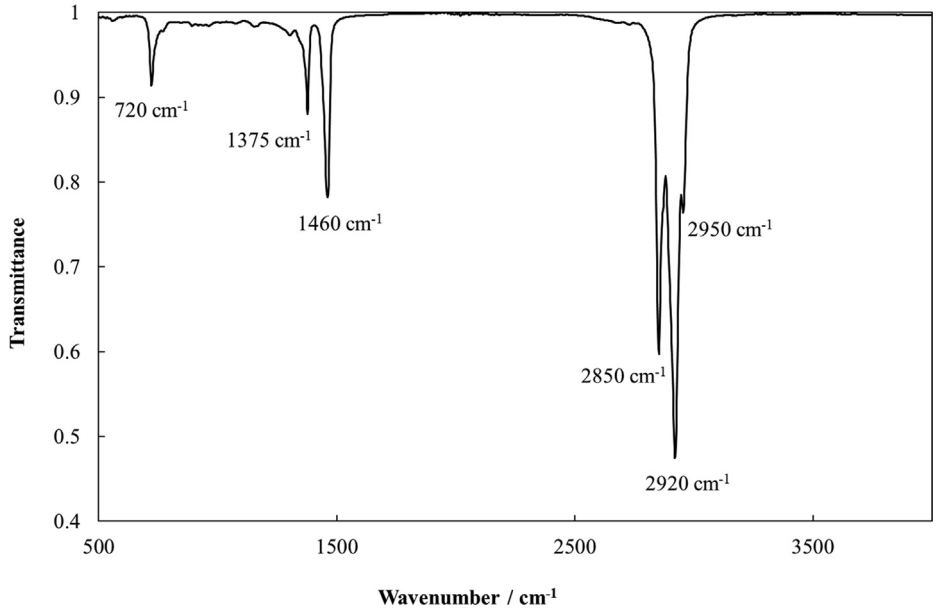

Fig. 1. FTIR spectrum of G-III base oil.

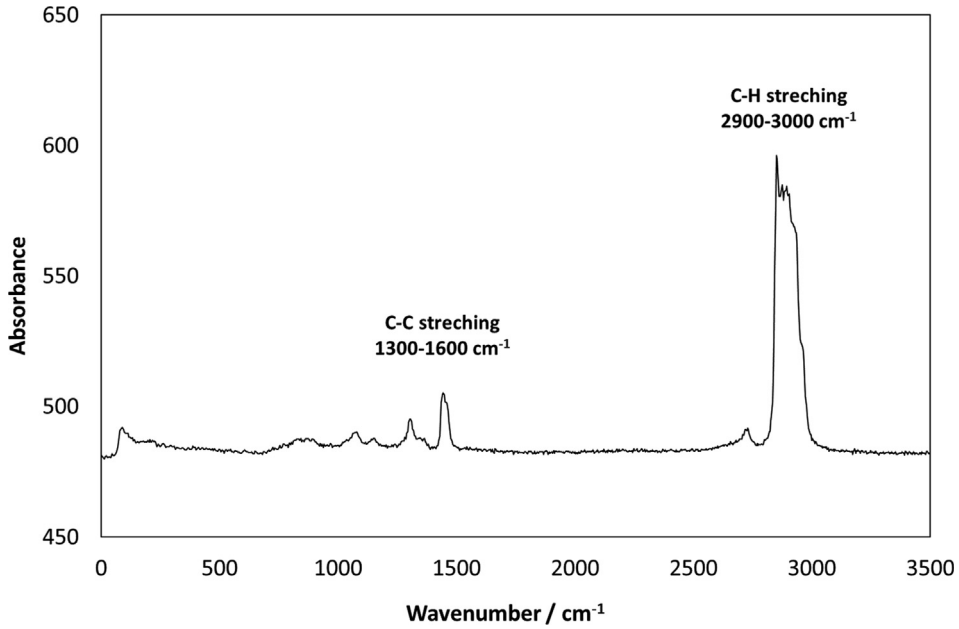

Fig. 2. Raman spectrum of G-III base oil.

heated T-PTD200 tribology cell, coupled to a MCR 302 rheometer from Anton Paar (Graz, Austria). The ball-on-three-plates setup is a well-established method for measuring both lubricated as well as dry tribological systems [32–36].

In this configuration, ball is fixed on a vertical shaft that is run by the rheometer motor whereas the pins, located at the bottom of the holder, are in contact with the ball forming an angle of 45° with the shaft. In every tribological test, the ball, supporting a vertical axial force exerted by the rheometer, rotates on the three pins. This axial force (20 N in this work) generates three normal forces (9.43 N each one) that act perpendicularly on the 3 pins surfaces. At each pin, the maximum Hertzian pressure is 1.1 GPa [37]. Specifically, in this work, cylindrical pins of 6 mm radius and 6 mm height, as well as 12.7 mm diameter balls, were used, both specimens made of hardened 100Cr6 steel (Rockwell C hardness: 62–66). The tests were completed at 213 rpm rotational speed (0.1 m s^{-1}), a duration of 3400 s and a temperature of 393.15 K. In each test, about 1.2 mL of lubricant was used, covering the contact surface for the entire duration of the friction test. T PTD 200 tribology cell guarantees precise alignment and therefore a homogeneous distribution of normal forces on the three plates. The same configuration was previously used by other authors in the field of lubricants [15,33,38–40]. The temperature has been chosen considering that for high performance of EV motors, a high-power density is needed, and therefore this increases the heat generation in the coil [41]. Nevertheless, to prevent demagnetization, the tem-

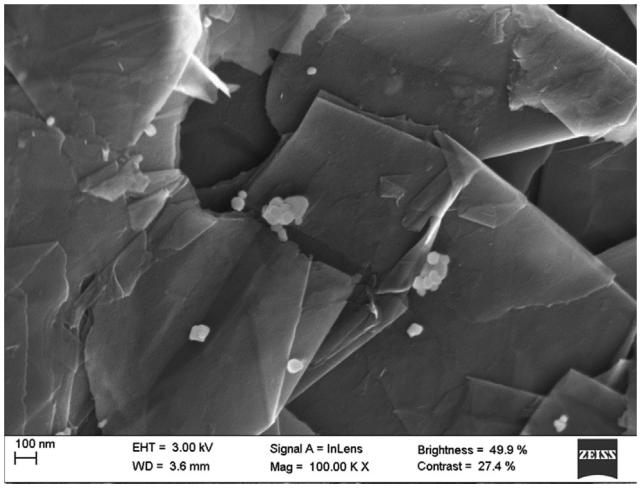

Fig. 3. SEM image of Mn_3O_4-Graphene nanocomposite.

perature should be lower than 150 °C or 110 °C depending on the literature [42,43]. More details can be found in a recent article of Rodriguez et al. [22].

Once the friction tests were carried out with each one of the studied lubricants (at least 3 replicates for each lubricant sample), the wear on each pin was evaluated, to find out which nanolubricant provides the best antiwear behavior. For this aim, a 3D profilometer (Sensofar, S-Neox) was used to quantify the wear through different parameters of the wear track: wear scar diameter (WSD), maximum wear track depth (WTD) and transversal area. It should be noted that these parameters were measured in the nine pins tested with each nanolubricant to acquire suitable average values (three pins per replicate). This 3D profiler was also employed to determine different roughness parameters (Ra, Rq, Rv, Rp, Rsk and Rku) of worn pins in order to quantify the antiwear capacity of each nanolubricant. For this purpose, the ISO4287 standard was employed making use of a Gaussian filter with a 0.08 mm cut-off. In addition, a confocal Raman microscope (WITec alpha300R+) was utilized to observe the worn scars of pins and obtain evidence about the chemical composition in the worn track and the tribological processes that may occur.

3. Results and analysis

3.1. Friction and wear results

The mean coefficients of friction (μ) obtained with the G-III base oil lubricants: neat oil and Mn_3O_4-G based nanolubricants, are presented in Table 1 and Fig. 7. It is observed that the use of any of the Mn_3O_4-G based nanolubricants almost varies the coefficient of friction in comparison to that obtained with the G-III base oil. In particular, the minimum friction coefficient was achieved with the 0.075 wt% Mn_3O_4-G nanolubricant (0.129 versus 0.135 found with the G-III base oil (Table 1).

As mentioned above, the wear produced in the pins during the friction tests was evaluated through three parameters of the wear scar: width, maximum depth, and transversal area. For this aim, cross section profiles of the wear scars of pins were extracted and 3D mapping of the wear tracks were taken (examples are presented in Figs. 8 and 9, respectively). The WSD, WTD and transversal area average values were obtained from the profiles of the wear scar on the pins lubricated with each G-III base oil lubricant and are reported in Table 1. It should be underlined that for all Mn_3O_4-G based nanolubricants, the three wear parameters (except for the WSD of 0.025 wt% Mn_3O_4-G nanolubricant) are much lower than those obtained with G-III base oil, especially in the case of transversal area. It is clear that the mass concentration of additives in the nanolubricant greatly affects the lubrication performance. The maximum reductions in width, depth and area have been reached with the G-III base oil + 0.075 wt% Mn_3O_4-G nanolubricant (Fig. 7), with reductions of 25, 50 and 64 %, respectively. Regarding balls, the wear was not evaluated.

Furthermore, in Table 1 it can be observed that with the constant increase in the Mn_3O_4-G concentration, wear parameters of the worn scar reduce till achieving the lowest values for the optimal mass concentration of 0.075 wt% Mn_3O_4-G. For G-III base oil + 0.100 wt% Mn_3O_4-G nanolubricant the wear increases considerably in comparison to the nanolubricant with the optimal concentration of 0.075 wt% Mn_3O_4-G. This fact may be due to when the concentration of additives increases, Mn_3O_4-G nanocomposites are more likely to agglomerate during friction tests, making it difficult for the nanocomposites to enter the tribological contact region, causing poorer lubrication performance.

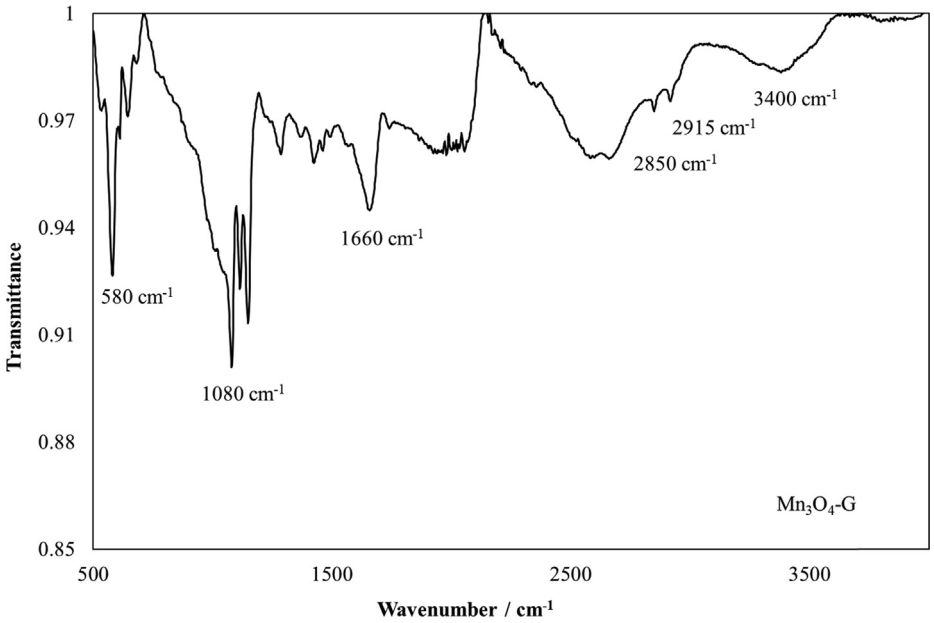

Fig. 4. FTIR spectrum of Mn_3O_4-G nanocomposite.

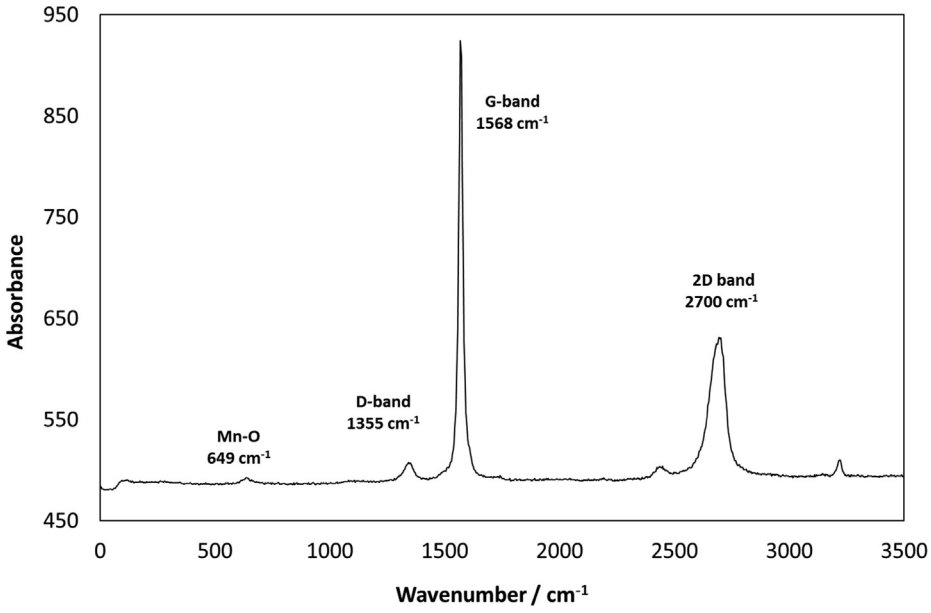

Fig. 5. Raman spectrum of Mn_3O_4-G nanocomposite.

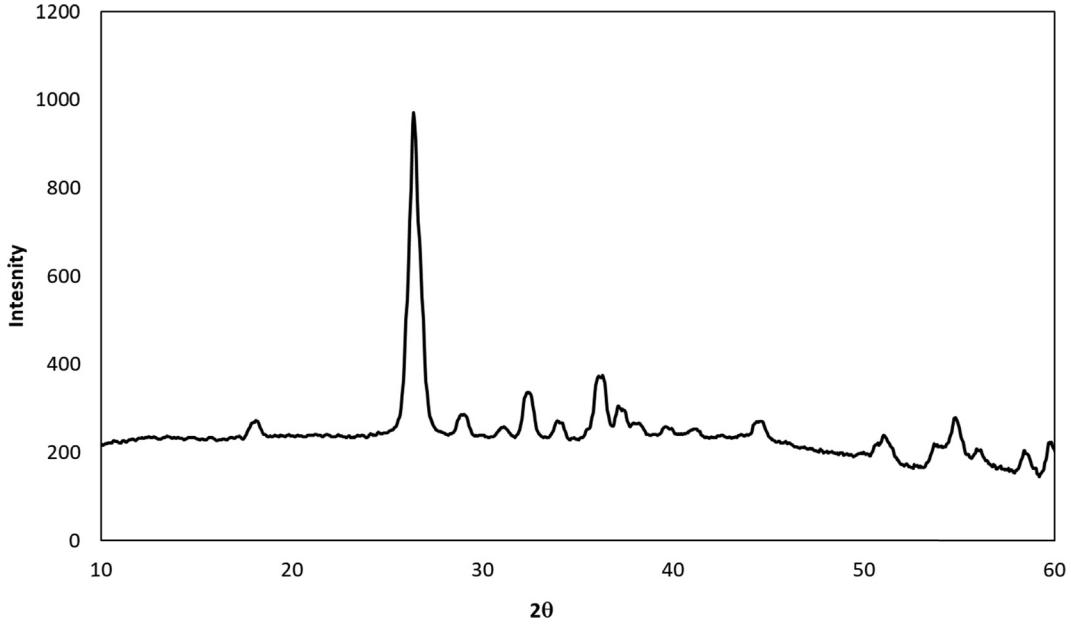

Fig. 6. XRD pattern of Mn_3O_4-G nanocomposite.

Table 1
Mean friction coefficients, μ, and mean wear parameters with their standard deviations for the studied G-III base oil lubricants at 393.15 K.

Sample	μ	σ	WSD/μm	σ/μm	WTD/μm	σ/μm	Area/ μm^2	σ/ μm^2
G-III base oil	0.1351	0.0014	366	18	2.11	0.19	607	44
+ 0.025 wt% Mn_3O_4-G	0.1318	0.0011	366	20	1.44	0.14	433	28
+ 0.050 wt% Mn_3O_4-G	0.1308	0.0010	313	16	1.43	0.16	357	32
+ 0.075 wt% Mn_3O_4-G	0.1295	0.0011	273	11	1.05	0.12	219	19
+ 0.100 wt% Mn_3O_4-G	0.1327	0.0012	356	15	1.91	0.14	462	33

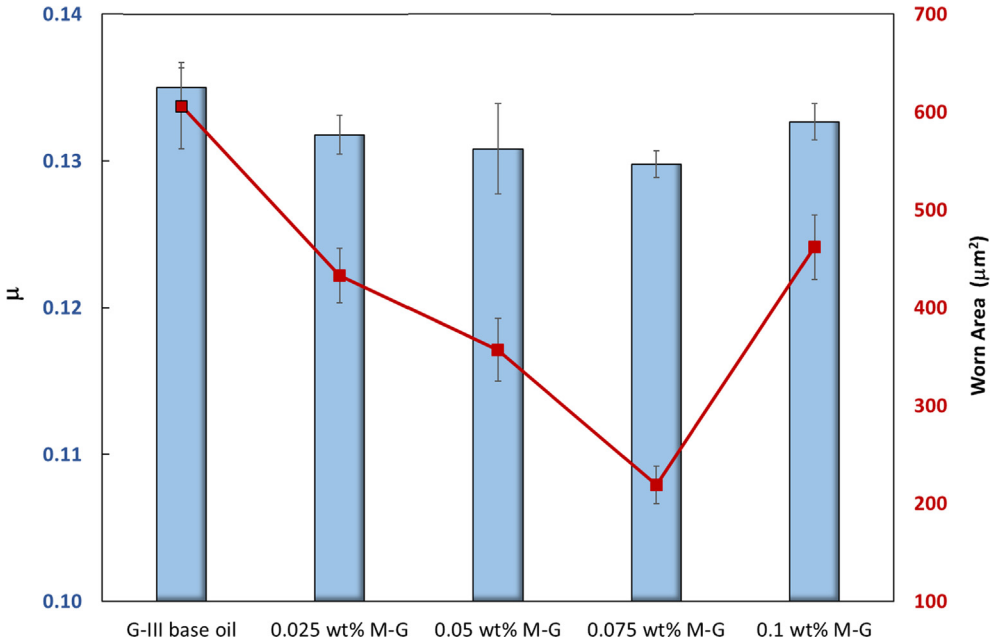

Fig. 7. Comparison between coefficients of friction (μ, bars) and worn areas (squares) obtained with G-III base oil and Mn_3O_4-G (M-G) based nanolubricants. Lines are just to guide eyes.

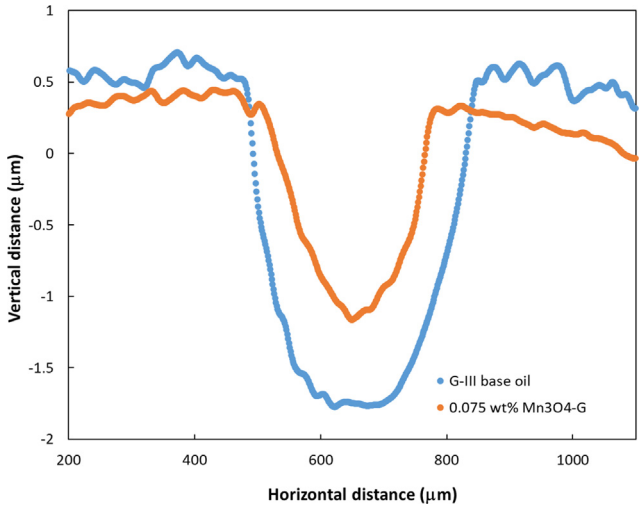

Fig. 8. Cross section profiles comparison of worn scars lubricated with G-III base oil and 0.075 wt% Mn_3O_4 based nanolubricant.

3.2. Tribological mechanisms

In order to find a possible tribological mechanism that explains the improved antiwear behavior of nanolubricants, roughness analysis, Raman mapping and SEM analysis on the worn tracks have been carried out.

Different roughness parameters in worn pins were investigated: arithmetic mean roughness value (Ra), root mean square roughness value (Rq), maximum peak-to-valley-height (Rv) and single highest peak above mean line (Rp). The obtained results (Table 2) showed that for all the roughness parameters, worn tracks lubricated with Mn_3O_4-G nanolubricants present lower roughness than those with G-III base oil (Table 2). For instance, a Ra value of 21.8 nm has been attained in the G-III base oil worn track whereas for the one lubricated with the G-III base oil + 0.075 wt% Mn_3O_4-G nanolubricant the littlest Ra (11.2 nm) was achieved that means a roughness decrease of 49%. It should be noted that, the unworn pin surface presented a much higher roughness with a Ra value of 93.4 nm. These obtained roughness results show that through the presence of the nanocomposites in the lubricant, after friction tests a more regular surface is obtained.

Nevertheless, two very different profiles can have the same mean roughness Ra. To draw conclusions, two other roughness parameters have been examined: skewness, Rsk, and kurtosis, Rku [44]. Skewness is a measure of asymmetry: Rsk > 0 indicates that the surface contains mainly peaks whereas Rsk < 0 if contains mainly valleys. This parameter is suitable for evaluating abrasion. Rku is a parameter associated with the geometry of the peaks and valleys, suitable for analyzing the degree of contact between the rubbing surfaces. Rku > 3 when the profile has a sharp height distribution whereas Rku < 3 implies a more uniform height distribution. Unlike skewness, the value of kurtosis does not distinguish between a peak and a valley in the profile [45]. As it can be observed in Table 2, for all the worn surfaces, Rsk < 0 and Rku < 3 which means plateau like worn surfaces with low both peaks and valleys (uniformly height distributed), because of the wearing process. As can be seen, Rsk values present a maximum value (*i.e.*, closer to zero, the value for a symmetric distribution about the mean line for a profile [44]) for the nanolubricant containing 0.075 wt% Mn_3O_4-G (optimum concentration minimizing friction and wear) whereas Rku roughly varies with concentration. Thus, it can be concluded that the wearing process leads to smoother surfaces, which could have a positive effect on the tribological performance of the nanolubricants because sliding friction could transform into rolling friction [46] due to the presence of spherical Mn_3O_4 NPs in the nanoadditive, while preventing direct contact between surfaces, and although the effect on friction is small, it has a large impact on antiwear capability at the optimum concentration (Table 1). In addition, during the friction process, graphene, 2D material also present in the nanocomposite, has an interlayer sliding effect to reduce attrition [47].

Furthermore, Raman spectra show that distinguishing areas appear in worn tracks of pins (Fig. 10). Blue areas are associated with the burned carbon from base oil [15], whereas red areas that

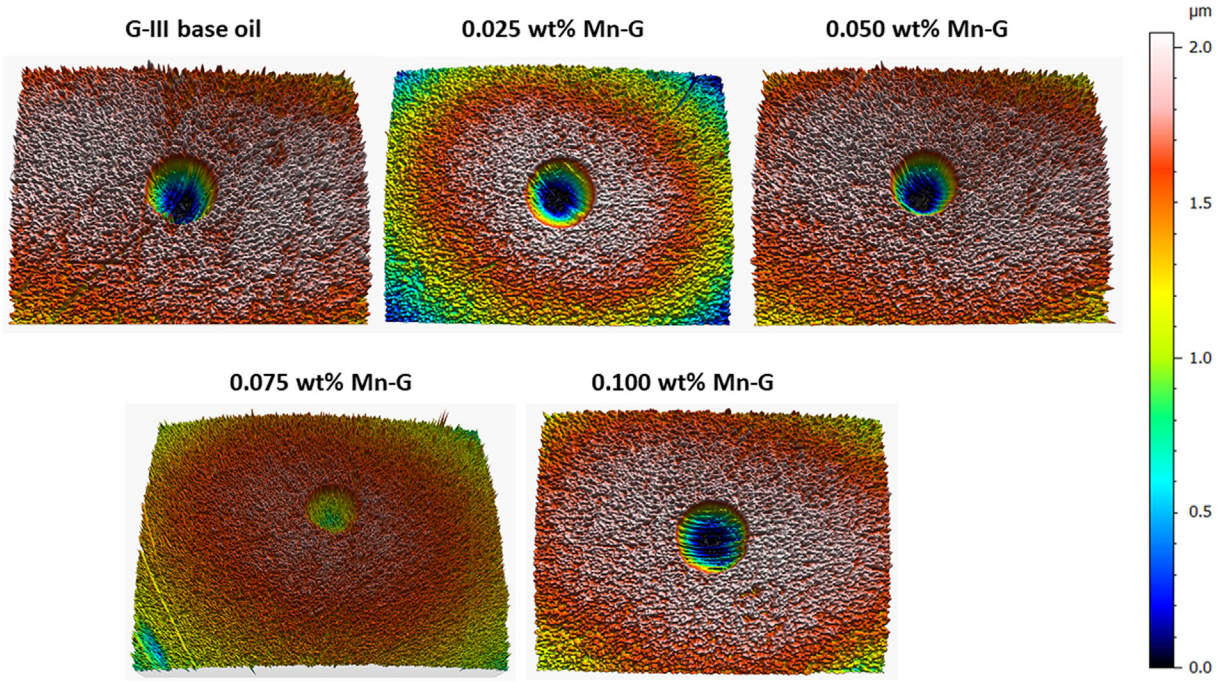

Fig. 9. 3D Surface topography of worn tracks lubricated with the designed G-III base oil lubricants.

Table 2
Different roughness parameters: Ra, Rq, Rp, Rv, Rsk and Rku with their uncertainties, σ, in worn pins lubricated with G-III base oil lubricants, Gaussian filter (0.08 mm cut-off).

Lubricant	Ra/nm	σ	Rq/nm	σ	Rp/nm	σ	Rv/nm	σ	Rsk	σ	Rku	σ
G-III base oil	21.8	2.2	27.4	2.7	39.6	3.8	45.3	4.2	−0.165	0.012	1.98	0.13
+ 0.025 wt% Mn_3O_4-G	17.7	1.5	22.1	1.8	34.8	3.5	39.6	4.5	−0.145	0.011	1.97	0.15
+ 0.050 wt% Mn_3O_4-G	14.9	1.7	17.5	1.9	33.4	2.7	32.1	2.6	−0.109	0.011	2.12	0.14
+ 0.075 wt% Mn_3O_4-G	11.2	1.1	10.2	1.3	16.7	1.1	19.6	1.3	−0.106	0.012	1.95	0.12
+ 0.100 wt% Mn_3O_4-G	16.4	1.3	19.5	1.4	34.1	3 0.3	37.3	3.3	−0.124	0.013	1.94	0.14

are placed along several furrows in the worn surface correspond to Raman peaks of the Mn_3O_4-G nanocomposite (D-band at 1354 cm^{-1} and G-band at 1595 cm^{-1} of graphene and Mn_3O_4 peak at 680 cm^{-1}). Therefore, a protective tribofilm from the Mn_3O_4-G is produced in the tribocontact [20]. It should be noted that the characteristic Raman band of Mn-O vibrations appearing at 649 cm^{-1} in the Mn_3O_4-G nanocomposite characterization (Fig. 5), after the friction tests this band in the worn track appears around 680 cm^{-1}. This shift evidence that most of the Mn_3O_4 was transformed into Mn_2O_3 under the generation of friction [20,48]. The chemical composition of Mn_3O_4 can be expressed as $MnO{\cdot}Mn_2O_3$, which suggests that during the friction tests, the temperature in the worn surface grew abruptly, the MnO is oxidized and transformed into a more stable Mn_2O_3 structure, contributing to its remarkable lubrication properties [20].

Moreover, the presence of graphene and Mn compounds in the tribofilm (Fig. 10) also demonstrates the synergistic protection of the nanocomposite. In friction tests, the graphene nanosheets can carry the Mn_3O_4 NPs and the latter can easily enter in the tribological contact zones [19]. Once in the contact zone, the Mn_3O_4 NPs can be released from the graphene sheets by the forces produced by friction and adsorbed in the contact surfaces, thus improving the tribological behavior of the lubricant. It should also be noted that graphene can slide layer by layer together with the rolling Mn_3O_4 NPs, hence achieving "slide-roll" effects in the tribological contact regions and reaching excellent tribological properties [19].

Moreover, energy dispersive X-Ray analysis in the worn scar lubricated with the optimal nanolubricant (0.075 wt% Mn_3O_4-G) was carried out to find the Mn element in the worn scar, finding that this element is present in a 0.40 wt% (Fig. 11). This fact confirms that the Mn_3O_4 forms a protective tribofilm in the tribological contact.

Finally, SEM images have been taken for the worn scars lubricated with the G-III base oil and with the different Mn_3O_4-G nanolubricants at different magnifications (Fig. 12). As can be observed, the main wear type for the neat base oil is two-body abrasive wear, the worn surface presenting ploughing [49]. Mild abrasion can be identified also in the worn tracks obtained with the nanolubricants, but in these cases when the nanocomposite concentration increases up to 0.075 wt%, smoother worn surfaces are achieved, dominating again abrasion for the highest concentration. This fact agrees with the roughness trend (Table 2). A possible explanation for this result could be attributed to the combined effect of both nanoadditives (with very different shapes) in the nanocomposite, graphene being a 2D material (easily sheared due to weak Van der Waals forces) whereas a spherical shape is the feature of Mn_3O_4 NPs (acting as ball bearings between the mating surfaces).

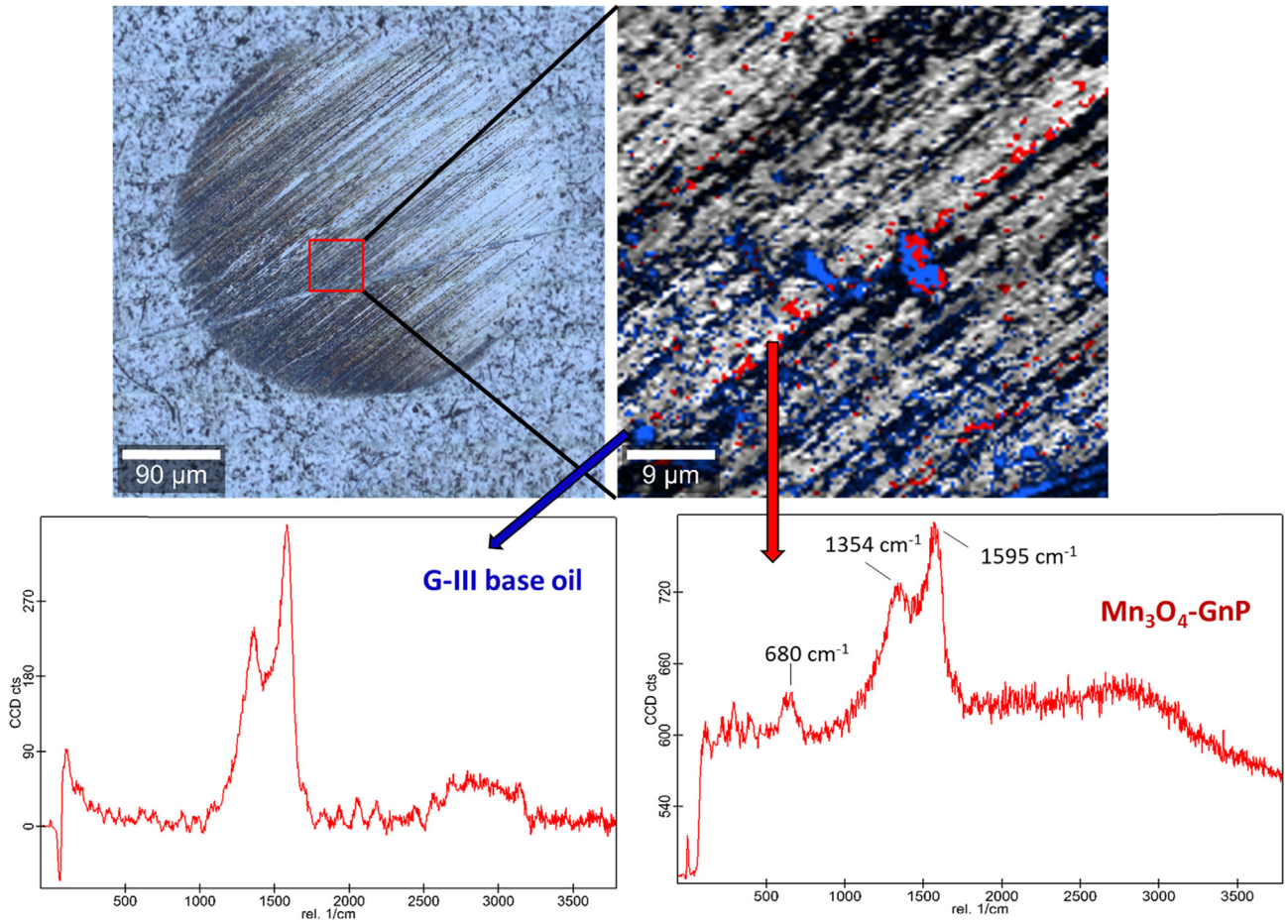

Fig. 10. Elemental mapping and Raman spectra of worn pins tested with 0.075 wt% Mn_3O_4-G nanolubricant.

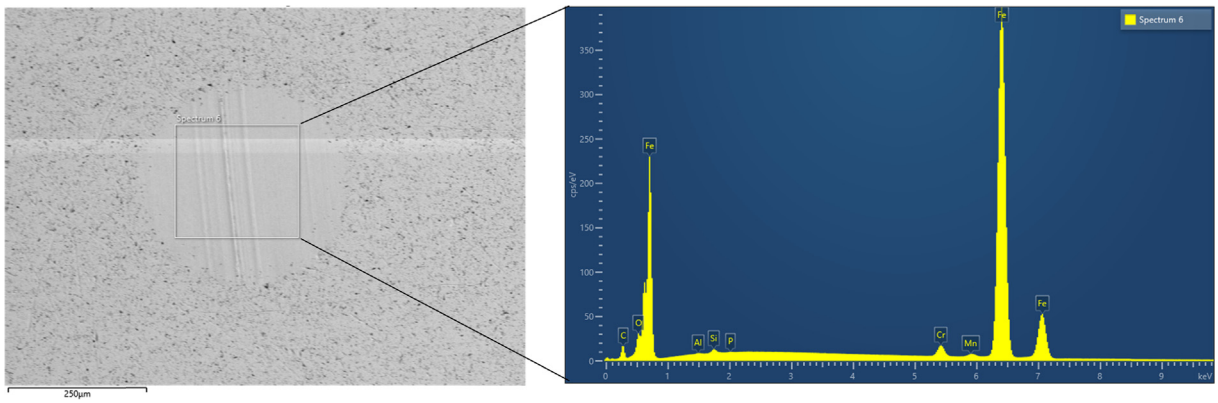

Element	Weight %
C	5.61
O	1.55
Si	0.27
P	0.03
Cr	1.55
Mn	0.40
Fe	90.43
Br	0.16
Total	100.00

Fig. 11. EDX spectra and elemental composition in the worn scar lubricated with 0.075 wt% Mn_3O_4-G nanolubricant.

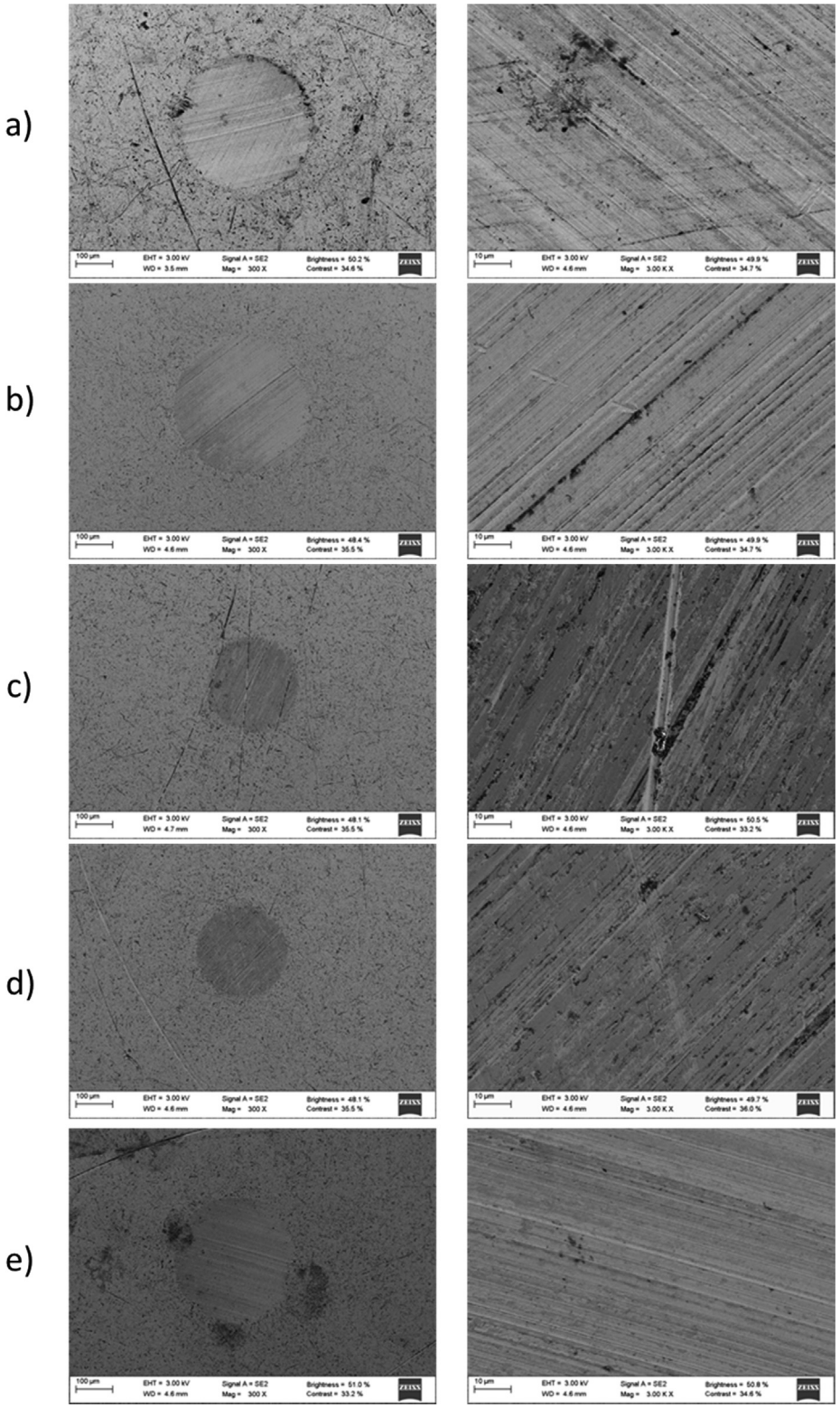

Fig. 12. SEM micrographs at two different magnifications of worn tracks lubricated with a) G-III base oil, b) G-III base oil + 0.025 wt% Mn_3O_4-G nanolubricant, c) G-III base oil + 0.050 wt% Mn_3O_4-G nanolubricant, d) G-III base oil + 0.075 wt% Mn_3O_4-G nanolubricant and e) G-III base oil + 0.100 wt% Mn_3O_4-G nanolubricant.

4. Conclusions

The conclusions of this research can be summarized as follows:

- Four nanolubricants based on a low viscosity oil (G-III base oil) were formulated, using Mn_3O_4-G nanocomposites as additives, characterizing the components by FTIR, Raman, XRD and/or SEM.
- Friction coefficients attained with the Mn_3O_4-G nanolubricants are slightly smaller than that observed for the non-additivated G-III base oil.
- For all the tribological tests carried out with Mn_3O_4-G nanolubricants the wear created in the pins is lower than that obtained using the G-III base oil with reductions up to 25, 50 and 64 % in width, depth, and area, respectively (G-III base oil + 0.075 wt% Mn_3O_4-G nanolubricant).
- Through the roughness, SEM and Raman analyses of worn tracks, it is evident that the lubrication mechanism can be explained by the adsorbed tribofilm of the graphene layers as well as the rolling effect of the Mn_3O_4 NPs.

CRediT authorship contribution statement

José M. Liñeira del Río: Writing – review & editing, Writing – original draft, Methodology, Investigation, Conceptualization. **Ramón Rial:** Writing – review & editing, Methodology, Investigation. **Enriqueta R. López:** Writing – review & editing, Validation, Supervision, Formal analysis, Conceptualization. **Josefa Fernández:** Writing – review & editing, Supervision, Project administration, Funding acquisition, Conceptualization.

Declaration of Competing Interest

The authors declare that they have no known competing financial interests or personal relationships that could have appeared to influence the work reported in this paper.

Acknowledgments

This research is supported by Xunta de Galicia (ED431C 2020/10), by the State Research Agency (AEI) of Spain and the European Regional Development Fund (ERDF, FEDER in Spanish) through the PID2020-112846RB-C22 project. JMLDR and RR are granted by the Program for the requalification, international mobility, and attraction of talent in the Spanish university system, modality Margarita Salas. Authors also thank Repsol Lubricants for supplying the G-III base oil and appreciate the support of the RIAIDT-USC analytical skills.

Appendix A. Supplementary material

Supplementary data to this article can be found online at https://doi.org/10.1016/j.molliq.2022.120271.

References

[1] K. Holmberg, A. Erdemir, The impact of tribology on energy use and CO_2 emission globally and in combustion engine and electric cars, Tribol. Int. 135 (2019) 389–396, https://doi.org/10.1016/j.triboint.2019.03.024.
[2] D. Sperling, Electric Vehicles: approaching the tipping point, in: D. Sperling (Ed.), Three Revolutions: Steering Automated, Shared, and Electric Vehicles to a Better Future, Island Press, Washington, DC, 2018, pp. 21–54, https://doi.org/10.5822/978-1-61091-906-7_2.
[3] K. Holmberg, P. Andersson, A. Erdemir, Global energy consumption due to friction in passenger cars, Tribol. Int. 47 (2012) 221–234, https://doi.org/10.1016/j.triboint.2011.11.022.
[4] Y.-A. Kwak, C.S. Cleveland, A. Adhvaryu, X. Fang, S. Hurley, T. Adachi, Understanding Base Oils and Lubricants for Electric Drivetrain Applications (2019).
[5] Y. Chen, S. Jha, A. Raut, W. Zhang, H. Liang, Performance characteristics of lubricants in electric and hybrid vehicles: a review of current and future needs, Frontiers in Mech. Eng. 6 (2020), https://doi.org/10.3389/fmech.2020.571464.
[6] S.C. Tung, M. Woydt, R. Shah, Global insights on future trends of Hybrid/EV driveline lubrication and thermal management, Frontiers in Mech. Eng. 6 (2020), https://doi.org/10.3389/fmech.2020.571786.
[7] L.I. Farfan-Cabrera, Tribology of electric vehicles: a review of critical components, current state and future improvement trends, Tribol. Int. 138 (2019) 473–486, https://doi.org/10.1016/j.triboint.2019.06.029.
[8] J.M. Liñeira del Río, E.R. López, J. Fernández, F. García, Tribological properties of dispersions based on reduced graphene oxide sheets and trimethylolpropane trioleate or PAO 40 oils, J. Mol. Liq. 274 (2019) 568–576, https://doi.org/10.1016/j.molliq.2018.10.107.
[9] W. Dai, B. Kheireddin, H. Gao, H. Liang, Roles of nanoparticles in oil lubrication, Tribol. Int. 102 (2016) 88–98, https://doi.org/10.1016/j.triboint.2016.05.020.
[10] D. Berman, A. Erdemir, A.V. Sumant, Graphene: a new emerging lubricant, Mater. Today 17 (2014) 31–42, https://doi.org/10.1016/j.mattod.2013.12.003.
[11] J.M. Liñeira del Río, M.J.G. Guimarey, M.J.P. Comuñas, E.R. López, J.I. Prado, L. Lugo, J. Fernández, Tribological and thermophysical properties of environmentally-friendly lubricants based on trimethylolpropane trioleate with hexagonal boron nitride nanoparticles as an additive, Coatings 9 (2019) 509, https://doi.org/10.3390/coatings9080509.
[12] G. Paul, S. Shit, H. Hirani, T. Kuila, N.C. Murmu, Tribological behavior of dodecylamine functionalized graphene nanosheets dispersed engine oil nanolubricants, Tribol. Int. 131 (2019) 605–619, https://doi.org/10.1016/j.triboint.2018.11.012.
[13] M.K.A. Ali, X. Hou, M.A.A. Abdelkareem, Anti-wear properties evaluation of frictional sliding interfaces in automobile engines lubricated by copper/graphene nanolubricants, Friction 8 (2020) 905–916, https://doi.org/10.1007/s40544-019-0308-0.
[14] M. Goodarzi, D. Toghraie, M. Reiszadeh, M. Afrand, Experimental evaluation of dynamic viscosity of ZnO–MWCNTs/engine oil hybrid nanolubricant based on changes in temperature and concentration, J. Therm. Anal. Calorim. 136 (2019) 513–525, https://doi.org/10.1007/s10973-018-7707-8.
[15] K.I. Nasser, J.M. Liñeira del Río, E.R. López, J. Fernández, Synergistic effects of hexagonal boron nitride nanoparticles and phosphonium ionic liquids as hybrid lubricant additives, J. Mol. Liq. 311 (2020), https://doi.org/10.1016/j.molliq.2020.113343 113343.
[16] W. Ahmed Abdalglil Mustafa, F. Dassenoy, M. Sarno, A. Senatore, A review on potentials and challenges of nanolubricants as promising lubricants for electric vehicles, Lubr. Sci. 34 (1) (2022) 1–29.
[17] M. Kalin, J. Kogovšek, M. Remškar, Mechanisms and improvements in the friction and wear behavior using MoS_2 nanotubes as potential oil additives, Wear 280–281 (2012) 36–45, https://doi.org/10.1016/j.wear.2012.01.011.
[18] https://www.narmaktrade.cz/en/products/base-oils/base-oil-yubase-6.
[19] J. Zhao, Y. Li, Y. He, J. Luo, In Situ Green Synthesis of the New Sandwichlike Nanostructure of Mn_3O_4/Graphene as Lubricant Additives, ACS Appl. Mater. Interfaces 11 (2019) 36931–36938, https://doi.org/10.1021/acsami.9b08993.
[20] B. Jin, G. Chen, J. Zhao, Y. He, Y. Huang, J. Luo, Improvement of the lubrication properties of grease with Mn_3O_4/graphene (Mn_3O_4#G) nanocomposite additive, Friction 9 (2021) 1361–1377, https://doi.org/10.1007/s40544-020-0412-1.
[21] Amit, R. Jamwal, S. Kumari, A.S. Dhaulaniya, B. Balan, D.K. Singh, Application of ATR-FTIR spectroscopy along with regression modelling for the detection of adulteration of virgin coconut oil with paraffin oil, LWT 118 (2020) 108754.
[22] E. Rodríguez, N. Rivera, A. Fernández-González, T. Pérez, R. González, A.H. Battez, Electrical compatibility of transmission fluids in electric vehicles, Tribol. Int. 171 (2022), https://doi.org/10.1016/j.triboint.2022.107544 107544.
[23] A. Baykal, Y. Köseoğlu, M. Şenel, Low temperature synthesis and characterization of Mn_3O_4 nanoparticles, J Open Chem. 5 (2007) 169–176, https://doi.org/10.2478/s11532-006-0064-7.
[24] X. Zhang, S. Wan, J. Pu, L. Wang, X. Liu, Highly hydrophobic and adhesive performance of graphene films, J. Mater. Chem. 21 (2011) 12251–12258, https://doi.org/10.1039/C1JM12087E.
[25] L. Yang, S. Cheng, X. Ji, Y. Jiang, J. Zhou, M. Liu, Investigations into the origin of pseudocapacitive behavior of Mn_3O_4 electrodes using in operando Raman spectroscopy, J. Mater. Chem. A 3 (2015) 7338–7344, https://doi.org/10.1039/C5TA00223K.
[26] Y. Hao, Y. Wang, L. Wang, Z. Ni, Z. Wang, R. Wang, C.K. Koo, Z. Shen, J.T.L. Thong, Probing layer number and stacking order of few-layer graphene by raman spectroscopy, Small 6 (2010) 195–200, https://doi.org/10.1002/smll.200901173.
[27] J.M. Liñeira del Río, M.J.G. Guimarey, M.J.P. Comuñas, E.R. López, A. Amigo, J. Fernández, Thermophysical and tribological properties of dispersions based on graphene and a trimethylolpropane trioleate oil, J. Mol. Liq. 268 (2018) 854–866, https://doi.org/10.1016/j.molliq.2018.07.107.
[28] A.C. Ferrari, J.C. Meyer, V. Scardaci, C. Casiraghi, M. Lazzeri, F. Mauri, S. Piscanec, D. Jiang, K.S. Novoselov, S. Roth, A.K. Geim, Raman spectrum of graphene and graphene layers, Phys. Rev. Lett. 97 (2006), https://doi.org/10.1103/PhysRevLett.97.187401 187401.

[29] S.-C. Weng, S. Brahma, P.-C. Huang, Y.-C. Huang, Y.-H. Lee, C.-C. Chang, J.-L. Huang, Enhanced capacity and significant rate capability of Mn3O4/reduced graphene oxide nanocomposite as high performance anode material in lithium-ion batteries, Appl. Surf. Sci. 505 (2020), https://doi.org/10.1016/j.apsusc.2019.144629 144629.
[30] Y. Fan, X. Zhang, Y. Liu, Q. Cai, J. Zhang, One-pot hydrothermal synthesis of Mn3O4/graphene nanocomposite for supercapacitors, Mater. Lett. 95 (2013) 153–156, https://doi.org/10.1016/j.matlet.2012.12.110.
[31] Y.-Z. Wang, T. Chen, X.-F. Gao, H.-H. Liu, X. Zhang, Liquid phase exfoliation of graphite into few-layer graphene by sonication and microfluidization, Mater. Express 7 (2017) 491–499, https://doi.org/10.1166/mex.2017.1395.
[32] P. Heyer, J. Läuger, A Flexible Platform for Tribological Measurements on a Rheometer 1027 (2008) 1168–1170, https://doi.org/10.1063/1.2964504.
[33] K. Shahrivar, A.L. Ortiz, J. de Vicente, A comparative study of the tribological performance of ferrofluids and magnetorheological fluids within steel–steel point contacts, Tribol. Int. 78 (2014) 125–133, https://doi.org/10.1016/j.triboint.2014.05.008.
[34] R. Gallego, T. Cidade, R. Sánchez, C. Valencia, J.M. Franco, Tribological behaviour of novel chemically modified biopolymer-thickened lubricating greases investigated in a steel–steel rotating ball-on-three plates tribology cell, Tribol. Int. 94 (2016) 652–660, https://doi.org/10.1016/j.triboint.2015.10.028.
[35] B.K. Bairgi, U.A. Mannan, R.A. Tarefder, Influence of foaming on tribological and rheological characteristics of foamed asphalt, Constr. Build. Mater. 205 (2019) 186–195, https://doi.org/10.1016/j.conbuildmat.2019.02.009.
[36] A.J.F. Bombard, J. de Vicente, Boundary lubrication of magnetorheological fluids in PTFE/steel point contacts, Wear 296 (2012) 484–490, https://doi.org/10.1016/j.wear.2012.08.012.
[37] P. Heyer, J. Läuger, Correlation between friction and flow of lubricating greases in a new tribometer device, Lubr. Sci. 21 (2009) 253–268, https://doi.org/10.1002/ls.88.
[38] K.K. Mishra, K. Panda, N. Kumar, D. Malpani, T.R. Ravindran, O.P. Khatri, Nanofluid lubrication and high pressure Raman studies of oxygen functionalized graphene nanosheets, J. Ind. Eng. Chem. 61 (2018) 97–105, https://doi.org/10.1016/j.jiec.2017.12.005.
[39] A. Beheshti, Y. Huang, K. Ohno, I. Blakey, J.R. Stokes, Improving tribological properties of oil-based lubricants using hybrid colloidal additives, Tribol. Int. 144 (2020), https://doi.org/10.1016/j.triboint.2019.106130 106130.
[40] J.P. Vallejo, J.M. Liñeira del Río, J. Fernández, L. Lugo, Tribological performance of silicon nitride and carbon black Ionanofluids based on 1-ethyl-3-methylimidazolium methanesulfonate, J. Mol. Liq. 319 (2020), https://doi.org/10.1016/j.molliq.2020.114335 114335.
[41] T. Ha, N. Han, M. Kim, K. Rho, D. Kim, Experimental study on behavior of coolants, Particularly the Oil-Cooling Method, in Electric Vehicle Motors Using Hairpin Winding, Energies 14 (2021) 956, https://doi.org/10.3390/en14040956.
[42] K.-H. Lee, H.-R. Cha, Y.-B. Kim, Development of an interior permanent magnet motor through rotor cooling for electric vehicles, Appl. Therm. Eng. 95 (2016) 348–356.
[43] P. Ponomarev, M. Polikarpova, J. Pyrhönen, Thermal modeling of directly-oil-cooled permanent magnet synchronous machine (2012).
[44] A. Kovalev, Z. Yazhao, C. Hui, Y. Meng, A concept of the effective surface profile to predict the roughness parameters of worn surface, Frontiers in Mech. Eng. 5 (2019), https://doi.org/10.3389/fmech.2019.00031.
[45] I. Hutchings, P. Shipway, Tribology: Friction and Wear of Engineering Materials, Butterworth-Heinemann, 2017.
[46] J. Padgurskas, R. Rukuiza, I. Prosyčevas, R. Kreivaitis, Tribological properties of lubricant additives of Fe, Cu and Co nanoparticles, Tribol. Int. 60 (2013) 224–232, https://doi.org/10.1016/j.triboint.2012.10.024.
[47] J. He, J. Sun, Y. Meng, X. Yan, Preliminary investigations on the tribological performance of hexagonal boron nitride nanofluids as lubricant for steel/steel friction pairs, Surf. Topogr. Metrol. Prop. 7 (2019), https://doi.org/10.1088/2051-672x/ab0afb 015022.
[48] A. Sukhdev, M. Challa, L. Narayani, A.S. Manjunatha, P.R. Deepthi, J.V. Angadi, P. Mohan Kumar, M. Pasha, Synthesis, phase transformation, and morphology of hausmannite Mn_3O_4 nanoparticles: photocatalytic and antibacterial investigations, Heliyon 6 (1) (2020) e03245.
[49] R.G. Bayer, Mechanical wear fundamentals and testing, Marcel Dekker Inc., New York (2004).